

Titan: Far-Infrared and Microwave Remote Sensing of Methane Clouds and Organic Haze

W. REID THOMPSON AND CARL SAGAN

Laboratory for Planetary Studies, Space Sciences Building, Cornell University, Ithaca, New York 14853

Received January 25, 1984; revised July 13, 1984

It is shown that Titan's surface and plausible atmospheric thermal opacity sources—gaseous N_2 , CH_4 , and H_2 , CH_4 cloud, and organic haze—are sufficient to match available Earth-based and Voyager observations of Titan's thermal emission spectrum. Dominant sources of thermal emission are the surface for wavelengths $\lambda \approx 1$ cm, atmospheric N_2 for 1 cm $\approx \lambda \approx 200$ μ m, condensed and gaseous CH_4 for 200 μ m $\approx \lambda \approx 20$ μ m, and molecular bands and organic haze for $\lambda \approx 20$ μ m. Matching computed spectra to the observed Voyager IRIS spectra at 7.3 and 52.7° emission angles yields the following abundances and locations of opacity sources: CH_4 clouds: 0.1 g cm^{-2} at a planetocentric radius of 2610–2625 km, 0.3 g cm^{-2} at 2590–2610 km, total 0.4 ± 0.1 g cm^{-2} above 2590 km; organic haze: $4 \pm 2 \times 10^{-6}$ g cm^{-2} above 2750 km; tropospheric H_2 : 0.3 ± 0.1 mol%. This is the first quantitative estimate of the column density of condensed methane (or CH_4/C_2H_6) on Titan. Maximum transparency in the middle to far IR occurs at 19 μ m where the atmospheric vertical absorption optical depth is ≈ 0.6 . A particle radius $\bar{r} \approx 2$ μ m in the upper portion of the CH_4 cloud is indicated by the apparent absence of scattering effects. © 1984 Academic Press, Inc.

INTRODUCTION

F. J. Low (1965) opened the era of Titan thermal infrared observations. His brightness temperature¹ (T_B) of $132 \pm 5^\circ K$ at 8 to 14 μ m (1250 to 710 cm^{-1}) was corroborated in a later measurement by Allen and Murdoch (1971) who found $T_B = 125^\circ K$ at 10 to 14 μ m (1000 to 710 cm^{-1}), and recognized the disagreement of their brightness temperature with the expected equilibrium temperature of roughly $80^\circ K$. Further work shortward of 14 μ m by Gillett *et al.* (1973), Low and Rieke (1974), and Gillett (1975) showed gaseous emission features by CH_4 , C_2H_6 , and C_2H_2 at these wavelengths. Thus, what was originally thought to be a high surface temperature caused by a greenhouse effect (Morrison *et al.*, 1972; Sagan, 1973; Pollack, 1973) turned out to be haze and molecular emission from a warm

mesosphere² (Danielson *et al.*, 1973; Caldwell, 1977). Measurements in the far-infrared and longward began with Morrison *et al.* (1972), who measured $T_B = 93 \pm 2^\circ K$ in the band at 16 to 28 μ m (620 to 360 cm^{-1}), and continued with Low and Rieke (1974) and McCarthy *et al.* (1980) between 15 and 35 μ m (670 to 290 cm^{-1}), Briggs (1974) and Jaffe *et al.* (1980) at centimeter wavelengths, Loewenstein *et al.* (1980) and Froidevaux and Ingersoll (1980) between 35 and 115 μ m (290 to 87 cm^{-1}), and Roellig *et al.* (1981) at 1 mm.

These measurements were obtained at a variety of facilities, from early measurements at mountaintop observatories and the National Radio Astronomy Observatory, to more recent observations using the

² The emitting region has traditionally been referred to as the stratosphere by many authors. The Voyager-derived temperature structure (see, e.g., Fig. 1) suggests defining the region of positive temperature gradient from 2625–2825 km as the stratosphere, while the near-isothermal region above 2825 km, from which most molecular and haze emission originates, is defined as the mesosphere.

¹ All brightness temperatures quoted here are those of the original authors adjusted to a standard Titan radius of 2575 km (Lindal *et al.*, 1983). Computed disk-integrated T_B 's are also normalized to this radius.

Kuiper Airborne Observatory, the Pioneer 11 spacecraft, the Very Large Array, and the Hale telescope on Palomar mountain. These measurements required great effort, given the weak thermal signal from Titan and the necessity, in many cases, of separating that signal from the stronger emission of nearby Saturn.

The general tendencies in thermal brightness deduced from these measurements are as follows: The centimeter and millimeter observations yield brightness temperatures near 90°K, while generally colder T_B 's, around 75 to 80°K, are observed between 115 and 35 μm . Brightness temperature increases shortward of 35 μm , passing again through 90°K around 15 μm . The highest T_B 's, around 130°K, are observed at shorter infrared wavelengths, around 10 μm .

Mesospheric emission models (Danielson *et al.*, 1973; Caldwell, 1977; McCarthy *et al.*, 1980) satisfactorily explained the Earth-based infrared observations in terms of thermal radiation from high altitude molecular sources, haze, and a cold surface or lower boundary. However, models which incorporated mesospheric emission plus a mild tropospheric greenhouse, such as the N₂/H₂/cloud model of Hunten (1978), were also consistent with these observations. Such models clearly demonstrated the *possibility* of the existence of a troposphere which extended below the cold lower boundary (taken to be a CH₄ cloud), to pressures and temperatures substantially higher than the tens to hundreds of millibars and 70–80°K required by the mesospheric emission models.

These ideas were borne out when the Voyager 1 infrared experiment (IRIS) obtained infrared spectra at many locations across Titan's disk. These spectra probed the atmosphere at several angles of emission with respect to the surface normal, making possible a much better determination of the vertical variation of opacity and temperature than could be obtained with Earth-based, disk-integrated spectra. Analysis showed that Titan infrared emission at

wavenumbers $\tilde{\nu} \approx 600 \text{ cm}^{-1}$ (wavelengths $\lambda \approx 17 \mu\text{m}$) originates, as expected, in the mesosphere (Hanel *et al.*, 1981). However, at $\tilde{\nu} \approx 600 \text{ cm}^{-1}$ ($\lambda \approx 17 \mu\text{m}$), mesospheric emission is superposed on a limb-darkened background (Hanel *et al.*, 1981; Samuelson *et al.*, 1981), indicating that emission in this part of the spectrum originates predominantly from the lower atmosphere, where temperature is increasing with depth (Tyler *et al.*, 1981). Voyager EUV measurements (Broadfoot *et al.*, 1981), the radio occultation experiment (Tyler *et al.*, 1981), and infrared observations (Hanel *et al.*, 1981) together showed N₂ to be the major atmospheric constituent, with a few percent of CH₄ and a spectroscopically undetected component of higher molecular mass (possibly Ar) inferred. Voyager infrared observations also revealed the presence of many simple organic compounds in Titan's atmosphere (Hanel *et al.*, 1981, 1982; Maguire *et al.*, 1981; Kunde *et al.*, 1981), products of ultraviolet and charged-particle synthetic processes in the upper atmosphere (Allen *et al.*, 1980; Strobel, 1982; Yung *et al.*, 1984; Sagan and Thompson, 1984), while Voyager EUV measurements (Smith *et al.*, 1982) detected a high altitude particulate haze between 3300 and 3600 km.

Samuelson *et al.* (1981) inverted IRIS spectra below 600 cm^{-1} , using a two-layer model to retrieve the optical depth in the mesosphere and troposphere as a function of frequency. They discovered about 0.2% H₂ and suggested liquid methane as a possible explanation of tropospheric opacity. Meanwhile, Thompson and Sagan (1981), Courtin (1982), and Hunt *et al.* (1983) computed emission spectra expected from Titan's atmospheric constituents, with opacity provided by collision-induced absorption by N₂ and CH₄. These studies, ranging from radio frequencies to the infrared, showed that, for $20 \mu\text{m} \leq \lambda \leq 1 \text{ cm}$, emitted radiation originates primarily from the lower atmosphere. Thompson and Sagan (1981) and Courtin (1982) noted a marginal discrepancy of the 1-mm observation

of Roellig *et al.* (1981) with predicted atmospheric brightness. Courtin (1982) and Hunt *et al.* (1983) pointed out the inability of models with N_2 and CH_4 gas opacities alone to reproduce the Titan T_B spectrum observed by Voyager IRIS. While Courtin (1982) compared the inferred optical depth profile of the unknown absorber to partial spectra of liquid and solid methane (Savoie and Fournier, 1970), Hunt *et al.* (1983) suggested the possible importance of other gas phase collision-induced opacity sources.

This paper is an extension to the studies summarized above. We use a more recent and more complete experimental liquid methane spectrum (Arning *et al.*, 1981), the spectral properties of laboratory-produced Titan organic haze, and collision-induced absorption of N_2 , CH_4 , and H_2 in conjunction with a radiative transfer technique to demonstrate that these constituents are sufficient to explain the Voyager observations. We derive the mole fraction of tropospheric H_2 , and the column density and limits on the altitude distribution of both methane cloud and organic haze.

METHODS

In order to produce model spectra, we specify the absorption properties of the atmosphere as a function of altitude and wavelength, and use these in a radiative transfer calculation to produce the expected emitted brightness as a function of wavelength and position on the disk (or emission angle). Collision-induced absorption by atmospheric gases (N_2 , and variable amounts of CH_4 , H_2 , and Ar) and by the CH_4 cloud; and absorption by laboratory-produced organic haze, which we call tholin, are considered. We stress that no component of this model is ad hoc; independent and adequate arguments exist for the presence of all of these materials in Titan's atmosphere. The opacity sources and atmospheric temperature–pressure–altitude structure employed in this study are shown in Fig. 1. In this figure we also preview our major results: quantities and locations of

opacity sources, which are derived and discussed in the following sections.

SPECTRAL PROPERTIES OF ATMOSPHERIC CONSTITUENTS

Collision-induced opacities are computed by the method of Birnbaum and Cohen (1976). The two adjustable parameters in their formalism are found by a least-squares fit of their spectral functions to the experimental data for N_2 , CH_4 and H_2 at the lowest temperatures available. For fits to collision-induced spectra of the linear molecules H_2 and N_2 , we add a term allowing for degeneracies arising from nuclear spin coupling in Eq. (25a) of Birnbaum and Cohen (1976). This results in multiplying their $(2J + 1)$ terms by 1 for even states and by 3 for odd states for hydrogen (with nuclear spin $\frac{1}{2}$) and multiplying $(2J + 1)$ by 6 for even states and by 3 for odd states for nitrogen (with nuclear spin 1).

The CH_4 spectrum at 195°K measured by Birnbaum (1975), the N_2 spectrum at 124°K measured by Buontempo *et al.* (1975), and the H_2 spectrum at 77.4°K measured by Birnbaum (1978) are used in the least-squares computational procedure. Fitting the spectra yields the two collisional time constants in the Birnbaum and Cohen formulation of collision-induced absorption.³ Since the product of the time parameters should be approximately inversely proportional to the temperature, in the absence of more definite information one may take the individual parameters to vary approximately as $T^{-0.5}$ (G. Birnbaum, private communication, 1983). Theoretical spectra are computed for every 1°K step in temperature over the range appropriate for Titan. These spectra provide the absorption due to gas-phase N_2 – N_2 , CH_4 – CH_4 , and H_2 – H_2 collisions. N_2 – CH_4 , CH_4 – N_2 , and H_2 – N_2

³ The values (in seconds) of the parameters (τ_1 , τ_2) obtained by this procedure, and subsequently used in computing spectra, are: H_2 (1.067×10^{-13} , 4.286×10^{-14}) at 77.4°K; N_2 (5.080×10^{-13} , 1.252×10^{-13}) at 124°K; CH_4 gas (8.697×10^{-14} , 6.029×10^{-14}) at 195°K; CH_4 liquid (4.493×10^{-14} , 7.878×10^{-14}) at 98°K.

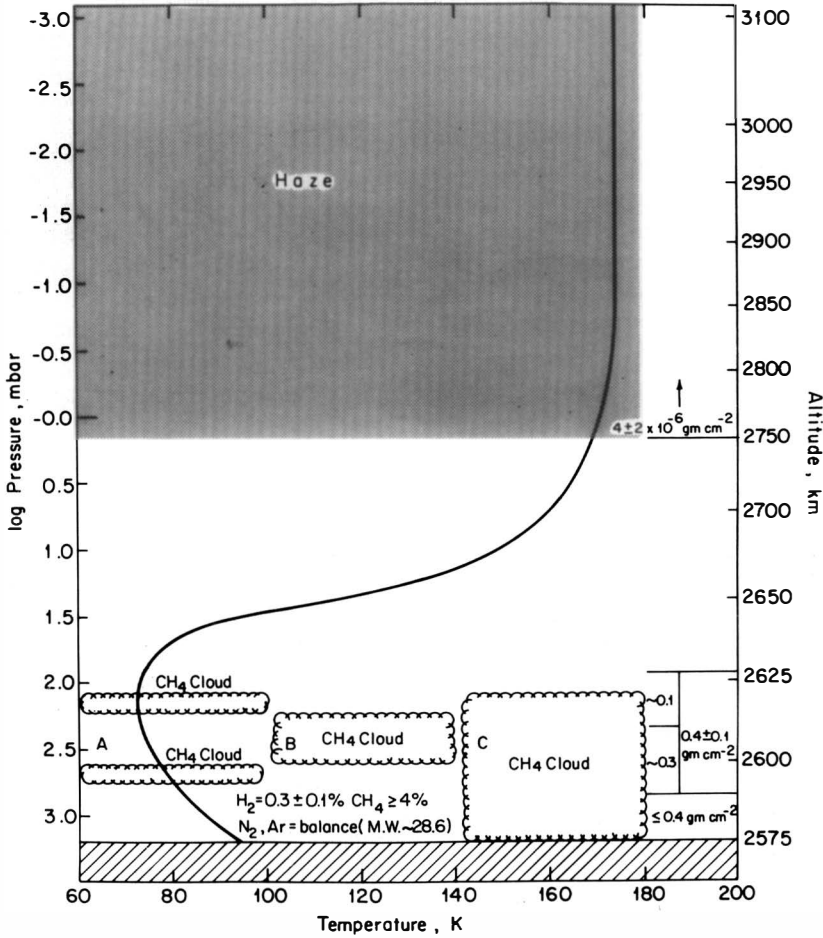


FIG. 1. Graphical summary of the location and abundance of cloud, organic haze, and gases in Titan's atmosphere. Haze location and column density are shown at top. The haze required by these models may be anywhere above about 2750 km. CH₄ cloud locations for Models A, B, and C are shown, as are the abundances of gases in the lower atmosphere. The general requirements of CH₄ cloud quantity and altitude are defined at lower right. See Table I and text for further explanation.

induced absorptions are calculated by the scaling relation of Ozier and Fox (1970), using the method discussed by Courtin (1982).⁴

Opacity from N₂-Ar and CH₄-Ar collisions is computed by scaling the N₂-N₂ and CH₄-CH₄ spectra, respectively, by a constant derived from experimentally observed

⁴ Magnetic tape copies of computed spectra over the spectral range 0.1–1000 cm⁻¹ and temperature range 60–180°K for gases (60–120°K for liquid CH₄), and/or Fortran programs used to compute the spectra, are available upon request from W. R. Thompson.

relative magnitudes of absorption due to homomolecular and heteromolecular collisions at low frequencies (Dagg *et al.*, 1974; Urbaniak *et al.*, 1976). H₂-Ar absorption is, at 195°K, very similar to that of H₂-N₂ (Kiss and Welsh 1959), so the opacity due to H₂-Ar collisions is handled by using the sum of the N₂ and Ar densities with the H₂-N₂ spectrum.

CH₄ liquid opacity is computed by a technique similar to that used for the gas. A least-squares fit of the Birnbaum and Cohen spectral functions is made to the best avail-

able liquid absorption spectrum (Arning *et al.*, 1981). While the density dependence of the liquid absorption spectrum is not expected to be exactly $\propto \rho^2$ because of the importance of multibody collisions in the liquid, error introduced here by the exclusion of higher order terms is small: Since the density of CH₄ under ambient Titan conditions is close to that employed in the laboratory measurements, the required extrapolation is minor. Although the low-pressure freezing point of CH₄ is 91°K and temperatures in Titan's atmosphere are as low as 73°K, the liquid CH₄ spectrum is a reasonable approximation to the spectrum of actual cloud condensate (see Discussion).

The optical properties (Khare *et al.*, 1984) of the complex organic solid synthesized by electrical discharge (and ultraviolet light) from a simulated Titan atmosphere composed of 91% N₂ and 9% CH₄ (Sagan and Khare, 1981), hereafter called Titan tholin (Sagan and Khare, 1979), are used in computing the haze absorption spectrum. The nature of such tholins is further discussed by Sagan *et al.*, 1984.

ATMOSPHERIC STRUCTURE

The Titan atmospheric temperature-pressure structure deduced by the Voyager IRIS and radio occultation experiments, as published in Samuelson *et al.* (1981), is used to define temperatures and densities for opacity computations. Atmospheric CH₄ content is variable, and is defined by an assumed fractional saturation at the surface, and a mole fraction limited, at altitudes where the temperature falls below the local CH₄ condensation temperature, by the vapor pressure. H₂ is uniform throughout the atmosphere at a chosen mole fraction. The mole fractions of N₂ and ³⁶Ar [the dominant argon isotope predicted by Owen (1982)] are adjusted dynamically, as the CH₄ mole fraction varies with altitude, to maintain a constant molecular mass of 28.6 Da—the molecular mass of the preferred atmospheric model of Samuelson *et al.* (1981). The condensed methane and Titan tholin mass fractions are arbitrarily variable

throughout the atmosphere, to 5-km resolution.

RADIATIVE TRANSFER

Radiative transfer calculations are made by numerical integration of the equation of transfer, $dI = \alpha(B - I) ds$, where I is the intensity at a particular frequency, B the Planck radiation function, α the linear absorption coefficient, ds the pathlength increment, and dI the incremental change in intensity over ds ($ds = dz/\mu$, where dz is the altitude increment and μ is the cosine of the angle between the ray path and the local planetary normal). The parameter α is computed by summing absorptions for all atmospheric components, with gas and particle densities varying with altitude, and collision-induced absorption determined from computed spectra appropriate to the local temperature. Temperature variation is accounted for in all spectra except that of Titan tholin, for which optical constants measured at room temperature are used. Atmospheric absorption/emission, surface emission, and surface reflection are considered. Atmospheric scattering is not included. (The implications of this approximation are considered below.) Numerical integration can then be performed along ray paths through the atmosphere, with atmospheric sphericity (and in fact emission from beyond the solid disk of the planet) included. Extension of radiative transfer calculations to radius $R = 3900$ km (pressure $p = 10^{-8}$ mbar) ensures inclusion of all significant thermal emission from the extended atmosphere. The stability and speed of the numerical computation are enhanced by integrating with a constant optical depth step size ($d\tau = \alpha ds$), independently for each surface emission angle (or radius from the center of the disk) considered. Polarization effects resulting from surface emission are also included, although they are averaged in the results shown here.

Models shown have surfaces of liquid CH₄. At wavelengths where the surface contributes significantly to emitted radiance (see *Surface Visibility* section), the re-

fractive indices of CH₄ and light ices such as H₂O and NH₃ are all low, leading to high emissivities ($\sim 0.97\text{--}0.99$) and similar thermal emission properties at temperatures appropriate to Titan's surface. Within the scope of the data available for comparison with computed results, the variation in thermal emission properties caused by the possible presence of C₂H₆ and N₂ in a liquid CH₄ surface is also negligible. While Titan tholin has a higher refractive index [~ 1.8 (Khare *et al.*, 1984)] and thus lower emissivity (~ 0.92), we find that models with tholin surfaces do not result in significantly different determinations of the quantity or location of opacity sources, within the error limits stated below.

RESULTS

BROAD-SPECTRUM COMPARISONS

Computed disk-integrated Titan brightness temperatures, for CH₄ and N₂ gas phase absorption only, over the broad spectral range 10^{-1} to 10^3 cm⁻¹ (10 cm to 10 μ m) are shown in Fig. 2. In a general sense, computed spectra for atmospheric gases only (solid line: 50% CH₄ surface saturation; broken line: 100% CH₄ surface saturation) match the *Earth-based* observations (points with error bars, all normalized to $R = 2575$ km) quite well. The notable exceptions are the measurements at $\log \tilde{\nu} = -0.11$ and 1.0 ($\lambda = 1.3$ cm and 1 mm). The error bars are so large for the 1.3 cm measurement that the center value (52°K) is off the graph, and disagreement here is not deemed significant. Although the 1-mm point is somewhat high, its lower bound misses the computed spectrum by only 3°K whereas the published 1.5- σ range (for $R = 2575$ km) is $95 \pm 13^\circ\text{K}$. Although the 1 mm point deserves further attention, there is no great discrepancy between predicted and Earth-based observations.

In contrast, predicted brightness is in definite disagreement with the *Voyager 1* average spectrum at emission angle $\theta = 52.7^\circ$ (jagged line, error $\sim \pm 0.1^\circ\text{K}$). [This

emission angle approximates the disk-integrated average in simple models of thermal emission, as noted by Courtin (1982).] It is seen that varying the gaseous CH₄ content of the lower atmosphere cannot bring the computed spectrum into accord with the observations. We are thus compelled to consider other plausible opacity sources: methane clouds, Titan tholin haze, and molecular hydrogen.

In Fig. 3 are shown wide-range spectra computed for models with atmospheric gases only, CH₄ clouds, and CH₄ clouds plus Titan tholin, but without hydrogen. The effects of CH₄ condensate, Titan tholin, and H₂ are discussed in detail later. The addition of CH₄ cloud opacity (line with single dashes) dramatically improves agreement with Voyager observations. The line with double dashes illustrates the effect of adding Titan tholin haze uniformly throughout the atmosphere at a mass fraction of 2×10^{-7} . Similar calculations define an upper limit for tropospheric organic haze mass fraction of $\sim 1 \times 10^{-7}$. (By "mass fraction" we always mean the fraction by mass of a given component relative to the total mass of the atmospheric parcel of which it is a part.)

That part of the spectrum below 50 cm⁻¹ ($\lambda > 200$ μ m) is little affected by liquid CH₄ opacity or by Titan tholin. Only changes in the atmospheric temperature structure, or the presence of materials not considered here which contribute opacity at low frequencies, can noticeably alter that part of the spectrum. We therefore proceed to a detailed discussion of the effects of CH₄ cloud, Titan tholin haze, and H₂ opacity on the computed Titan emission spectrum in the frequency range 200 to 600 cm⁻¹, where changes in computed spectra can be compared directly with Voyager IRIS observations.

COMPARISONS WITH VOYAGER IRIS OBSERVATIONS

The use of average Voyager spectra for emission angles $\theta = 52.7$ and 7.3° (Samuelson *et al.*, 1981) allows us to investi-

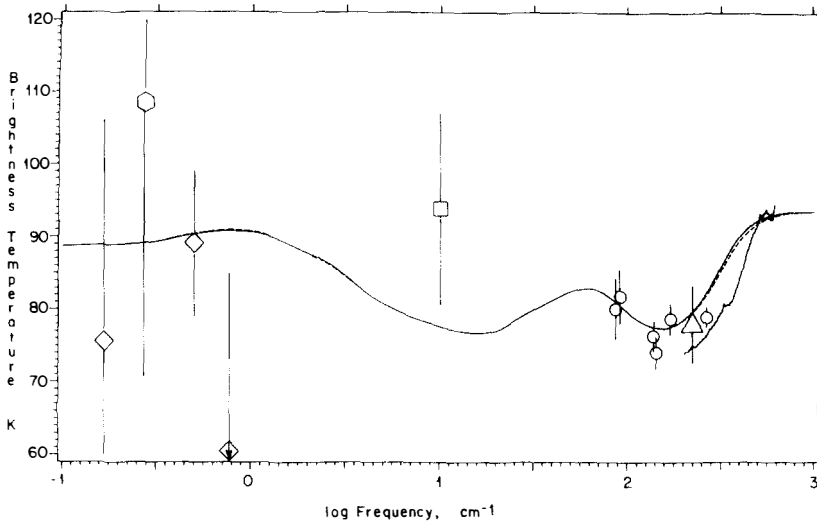


FIG. 2. Observed and computed brightness temperature (T_B) spectra for Titan's atmosphere from 0.1 to 1000 cm^{-1} (10 cm to 10 μm). Smooth unbroken curve: disk-integrated computed spectrum of gaseous N_2 and CH_4 for 50% CH_4 saturation at the surface. Dashed curve: 100% CH_4 surface saturation. Jagged line from 200 to 600 cm^{-1} : Voyager 1 spectrum for 52.7° average emission angle (Samuelson *et al.*, 1981). Points: Earth-based observations normalized to a common radius of 2575 km. \circ : Briggs (1974); \diamond : Jaffe *et al.* (1980) (diamond with arrow should be located at $T = 52^\circ\text{K}$); \square : Roellig *et al.* (1981); \circ : Loewenstein *et al.* (1980); \triangle : Froidevaux and Ingersoll (1980). Thermal emission from collision-induced transitions of atmospheric N_2 and CH_4 dominates Titan's spectrum over most of the four-decade range in frequency shown (see text). Variation of the atmospheric CH_4 content has little effect on the computed surface/atmosphere thermal emission spectrum, which is too hot from 200 to 500 cm^{-1} and somewhat too cold at 10 cm^{-1} (1 mm).

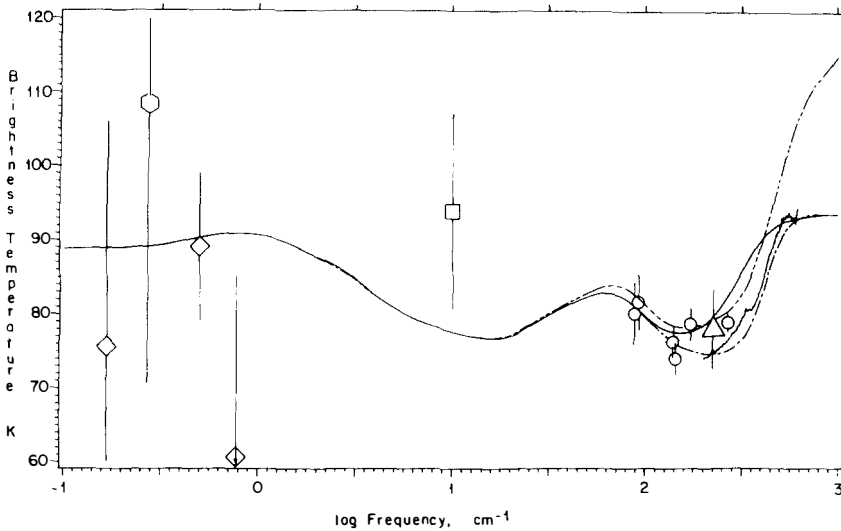


FIG. 3. Observed and computed T_B spectra for Titan's atmosphere. The unbroken curve is the emission spectrum computed for gaseous N_2 and CH_4 , with 50% CH_4 surface saturation. Points and jagged curve are Earth-based and Voyager 1 observations respectively (see Fig. 2 caption). The single-dashed curve shows the dramatic improvement in agreement of computed and observed spectra which results from the addition of CH_4 cloud opacity in the upper troposphere (mass fraction $\approx 3 \times 10^{-4}$), while the double-dashed curve shows the consequences of adding too much haze (here uniformly distributed at mass fraction 2×10^{-7}) to the atmosphere. The upper limit of tropospheric haze mass fraction is $\sim 1 \times 10^{-7}$.

gate how atmospheric opacity models reproduce both the spectral shape and the observed limb darkening or brightening from 200 to 600 cm^{-1} . In Figs. 4–7 are shown, respectively, the computed emission of major atmospheric gases ($\text{N}_2 + \text{CH}_4 + \text{Ar}$) alone, and of these constituents plus varying amounts of H_2 , CH_4 clouds, and Titan tholin haze added individually.

Gas opacity of N_2 , CH_4 and Ar alone (Fig. 4) results in a computed T_B which is much higher than that observed by Voyager below 500 cm^{-1} , as noted previously. The opacity of N_2 , dominant at lower frequencies, has nearly disappeared (see curve with 0% CH_4). Increase of the percent saturation of CH_4 at the surface produces a favorable change in the computed spectra. However, continued increase above about 35% saturation (about 0.04 mole fraction) has little effect because the gas phase CH_4

abundance is limited, at the higher altitudes, by vapor pressure. Since 35% saturation at the surface corresponds to condensation at ~ 2600 km, further increase of CH_4 saturation adds opacity only very near the surface, and thus produces little incremental change in the T_B spectra except at frequencies where the CH_4 gas above the saturation altitude is nearly transparent.

The addition of H_2 (Fig. 5) introduces substantial atmospheric opacity through most of the spectral interval 200 to 600 cm^{-1} , and enhances limb darkening (not shown here) since emission is now biased toward the lower atmosphere at all frequencies. H_2 mole fractions $\sim 10^{-3}$ substantially decrease surface visibility, which is high at $\bar{\nu} > 500$ cm^{-1} in the absence of absorbers other than N_2 and CH_4 . Although H_2 alone does decrease T_B and shows some potential in helping match the observed inflection

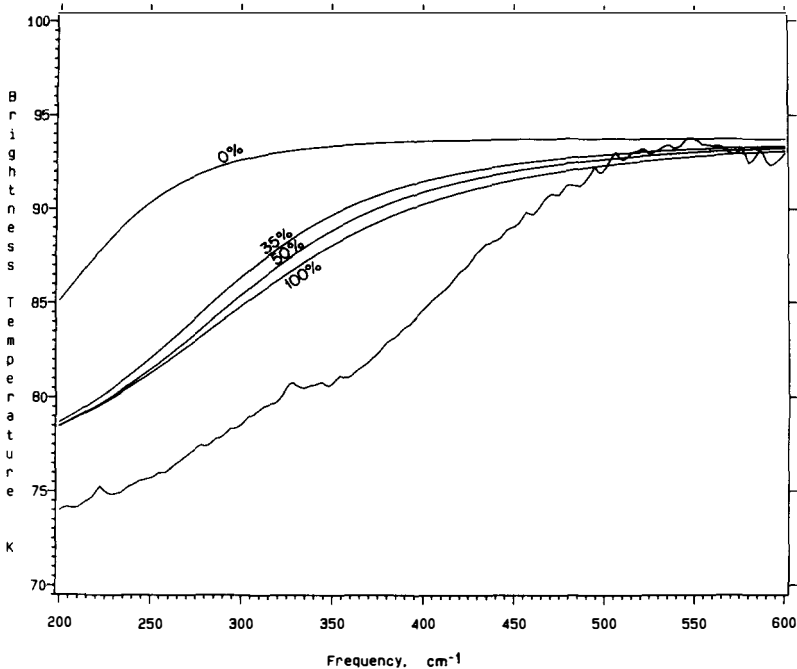


FIG. 4. Variation of the Titan T_B spectrum from 200 to 600 cm^{-1} at 52.7° emission angle, with atmospheric CH_4 content. Irregular line is the average Voyager 1 52.7° spectrum (Samuelson *et al.*, 1981). Smooth curves are computed emission spectra for atmospheric N_2 and CH_4 . Curves are labeled with values of CH_4 surface saturation. Increase of atmospheric CH_4 improves agreement with, but cannot alone match, the observed spectrum.

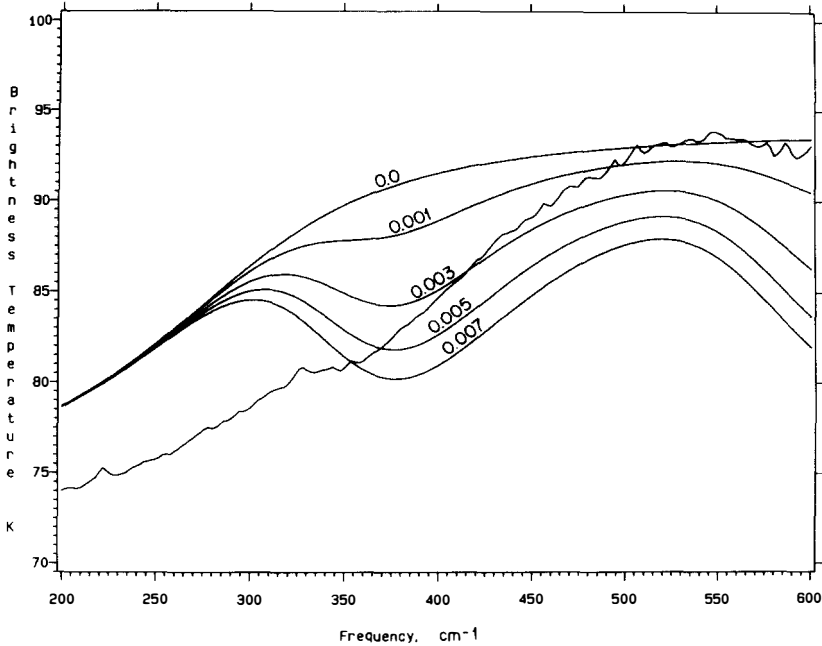


FIG. 5. Variation of the Titan T_B spectrum at 52.7° emission angle with atmospheric H_2 abundance. In all cases N_2 and CH_4 are present, with a CH_4 surface saturation of 35%. Smooth curves are computed spectra, labeled with the H_2 mole fraction. The irregular line is the average Voyager 1 spectrum. H_2 may help explain the curve inflection at $\sim 350\text{ cm}^{-1}$, but does not alone affect the computed spectrum in the desired fashion at lower frequencies.

near 360 cm^{-1} , combinations of N_2 , CH_4 , and H_2 gases are insufficient to reproduce the Voyager spectra.

The addition of CH_4 cloud opacity (Fig. 6) produces a trend of just the type needed to match the observations. The overall slope of the spectrum can be readily matched, since liquid methane opacity is falling from a maximum near 150 cm^{-1} and naturally reproduces the roughly sigmoid shape observed. The major discrepancies are the failure of liquid CH_4 alone to reproduce the observed near-inflection at 330 to 370 cm^{-1} , and the tendency of the computed spectrum to underestimate substantially the 1 to 2°K limb darkening observed below about 500 cm^{-1} (see discussion of limb darkening below).

The addition of Titan tholin to the atmosphere (Fig. 7) causes limb brightening and increases T_B when the tholin is located in the mesosphere. Organic haze production

is expected to be substantial in these regions of Titan's atmosphere (Allen *et al.*, 1980; Sagan and Thompson, 1984), and Smith *et al.* (1982) have observed high altitude haze between 3300 and 3600 km.

The success of liquid methane in matching the major trend of the Voyager spectrum is satisfying, but the further addition of H_2 and organic haze in rather well-defined quantity and location can reproduce all of the major features in the observed Titan spectra. In obtaining this match, the amount of H_2 (assumed uniformly distributed), and the amount and altitude distribution (to 5-km resolution) of liquid CH_4 and Titan tholin are allowed to vary. Once the best-fit solutions are obtained, the maximum excursion of each parameter is estimated by varying it, while holding all other parameters constant, until the mean-square deviation of the fit approximately doubles. This procedure defines the volume in pa-

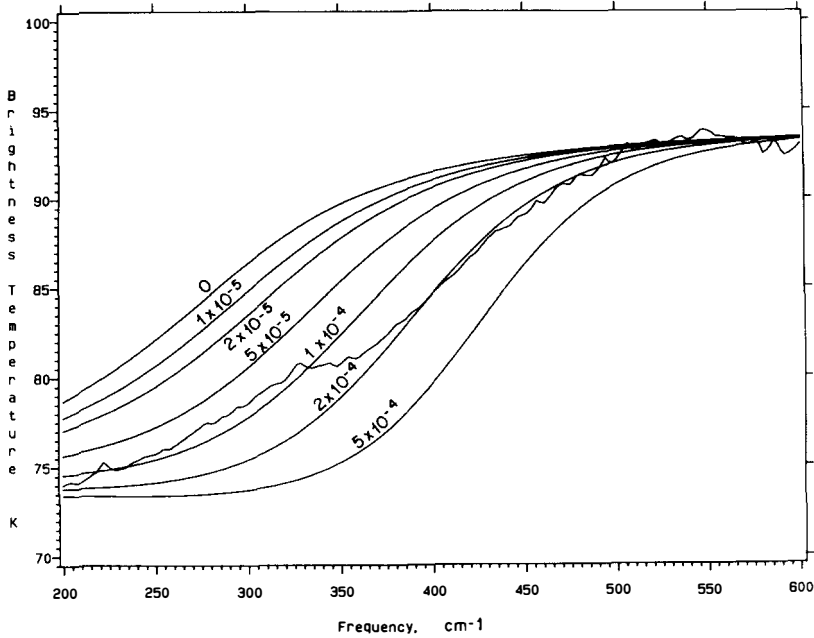


FIG. 6. Variation of the Titan T_B spectrum at 52.7° emission angle with CH_4 cloud density. In all cases N_2 and CH_4 are present, with a CH_4 surface saturation of 35%. Smooth curves are the computed spectra, while the irregular line is the average Voyager 1 spectrum. Curves are labeled with the CH_4 cloud mass fraction, which in all cases is constant below 2620 km to the surface and zero above 2620 km. [To convert from mass fraction to total column density (g cm^{-2}) for this distribution, multiply by 1.1×10^4 .] Although additional components are required to match the spectrum across the whole frequency range, a CH_4 cloud is crucial for the reproduction of the overall slope and shape of the observed spectrum. The CH_4 cloud is the single most important opacity source other than atmospheric gases in Titan's troposphere.

parameter space of solutions deviating from the observed spectra by no more than about twice the mean-square deviation of the "best fit."

BEST MODELS: LIMB DARKENING AND QUANTITATIVE DETERMINATIONS

Three of the best fits obtained are shown in Fig. 8. In all cases the H_2 mole fraction is 0.003 and haze (Titan tholin) is present uniformly in the near-isothermal region of the atmosphere, at a temperature $\sim 174^\circ\text{K}$, from 2840 km upward. In Model A, the Titan tholin mass fraction is 2.5×10^{-6} and methane cloud is present between 2615 and 2620 km at mass fraction 5.2×10^{-4} , and from 2595 to 2600 km at mass fraction 2.3×10^{-4} . In Model B, the Titan tholin mass fraction is 2.5×10^{-6} and CH_4 cloud is dis-

tributed from 2600 to 2615 km at mass fraction 2.0×10^{-4} . In Model C the Titan tholin mass fraction is 3.0×10^{-6} and CH_4 cloud is uniformly present at a mass fraction of 1.0×10^{-4} from 2620 km to the surface (2575 km). Two-layer models (such as Model A) fit the observed spectra slightly better than uniform distributions near T_{\min} (such as Model B), primarily because the slope and limb darkening below 300 cm^{-1} are better reproduced. Uniform distributions extended further toward the surface as in Model C tend to require more haze to offset a general flattening of the spectrum, which in turn produces an undesirable general decrease in limb darkening. Remaining differences between these models and the Voyager spectra are considered in the Discussion.

1. H_2 and Organic Haze

Extensive testing as previously outlined shows that the limits on H_2 mole fraction and haze column density are well determined: 0.003 ± 0.001 and $4 \pm 2 \times 10^{-6} \text{ g cm}^{-2}$, respectively. These values are coupled—an increase of H_2 produces strong absorption in the high frequency half of the spectrum, which must be compensated by high-altitude haze. However, haze drastically affects limb darkening, producing an unacceptable convergence of the 7.3° and 52.7° spectra when present at column densities above $6 \times 10^{-6} \text{ g cm}^{-2}$. In Fig. 9 are shown the qualitative and quantitative effects of varying haze column density. The haze upper limit in turn places an upper limit of about 0.004 on the H_2 mole fraction, while decrease of H_2 below about 0.002 mole fraction results in a failure of the spec-

trum to agree with observations from about 230 to 370 cm^{-1} . Effects of the variation of H_2 content are shown in Fig. 10.

The Titan tholin vertical distribution is confined to the upper atmosphere primarily because the amount required to reproduce the observed T_B near 550 cm^{-1} would destroy the observed limb darkening if located through a region of decreasing temperature lower in the atmosphere. However, the admixture of Titan tholin at about 10^{-7} mass fraction in the region of the CH_4 cloud is allowed, although not required. This would make the tholin column density in the lower atmosphere possibly much greater than that in the upper atmosphere, as much as $\sim 10^{-3}$ of the CH_4 column density or $\sim 5 \times 10^{-4} \text{ g cm}^{-2}$.

There is no specific feature of the Titan tholin spectrum which is needed to reproduce localized structure in the IRIS spec-

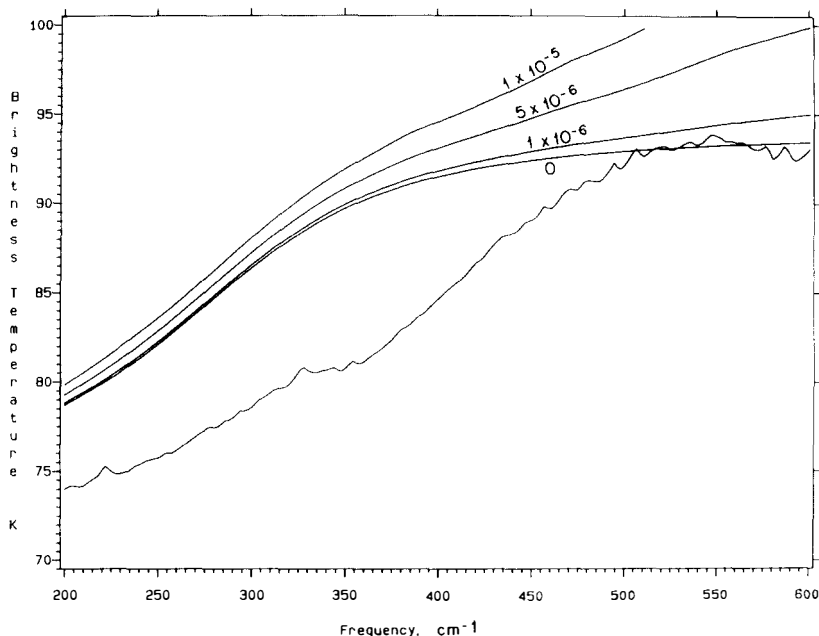


FIG. 7. Variation of the Titan T_B spectrum at 52.7° emission angle with organic haze (Titan tholin) content. In all cases N_2 and CH_4 are present, with a CH_4 surface saturation of 35%. Smooth curves are computed spectra, while the irregular line is the average Voyager 1 spectrum. Curves are labeled with the haze mass fraction, which in all cases is constant above 2840 km and zero below 2840 km. [To convert from mass fraction to total column density (g cm^{-2}) for this distribution, multiply by 1.7.] High-altitude haze produces a general brightening which increases rapidly with frequency above $\sim 350 \text{ cm}^{-1}$.

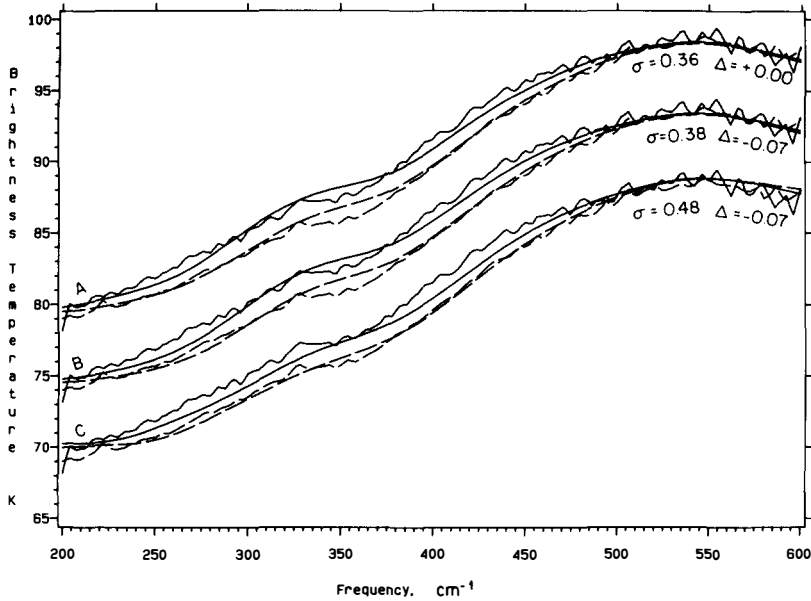


FIG. 8. Titan T_B spectra at 7.3° (solid lines) and 52.7° (dashed lines) emission angles. Lines with detailed structure are Voyager 1 averaged spectra (Samuelson *et al.*, 1981). Smooth curves are computed spectra for Models A, B, and C. Top and bottom sets of curves are offset by $+5^\circ\text{K}$ and -5°K , respectively. In all models haze is present only above 2840 km, and H_2 is present at a mole fraction of 0.003. In A, haze mass fraction is 2.5×10^{-6} and CH_4 cloud is present at 5.2×10^{-4} mass fraction between 2615 and 2620 km, and at 2.3×10^{-4} mass fraction between 2595 and 2600 km. In B, haze mass fraction is 2.5×10^{-6} and CH_4 cloud is present at 2.0×10^{-4} mass fraction between 2600 and 2615 km. In C, haze mass fraction is 3.0×10^{-6} and CH_4 cloud is present at 1.0×10^{-4} mass fraction from 2620 km downward to the surface at 2575 km. σ is the average RMS temperature deviation ($^\circ\text{K}$) of the computed from the observed curves. Δ is the average temperature difference ($^\circ\text{K}$) between the computed and the observed curves. ("Average" means the deviations for the 7.3 and 52.7° curves are computed independently and then averaged.) Models A and B, with cloud absent below 2590 km, are slightly preferred.

tra. Any material which has, as Titan tholin does, a roughly constant imaginary part of the refractive index (n_i) through this spectral range will show an approximately linear dependence of absorption coefficient on frequency. If Titan haze is similar to Titan tholin, as we expect, the column density required by the model may be taken literally. Otherwise, the column density will scale linearly with the ratio of Titan tholin n_i (Khare *et al.*, 1984) to that of the actual haze material.

2. CH₄ Cloud: Quantity and Location

CH_4 cloud column density above the 2590-km level is constrained to a maximum of about 0.5 g cm^{-2} (Fig. 11). Quantities

larger than this produce an unacceptable flattening of the spectral shape and premature disappearance of limb darkening below about 300 cm^{-1} , primarily because limb darkening produced by atmospheric and cloud opacity at lower altitudes, where the temperature gradient is highest, is masked. The lower limit is set by the necessity of having sufficient cloud material near $T_{\min} \approx 73^\circ\text{K}$ to produce brightness temperatures as low ($\sim 74^\circ\text{K}$) as those observed. The CH_4 condensate column density required is then $0.4 \pm 0.1 \text{ g cm}^{-2}$.

As already noted, the requirement of low T_B 's near 200 cm^{-1} and the successful reproduction of spectral slope and limb darkening constrain the possible vertical distributions of condensed CH_4 . A distribution

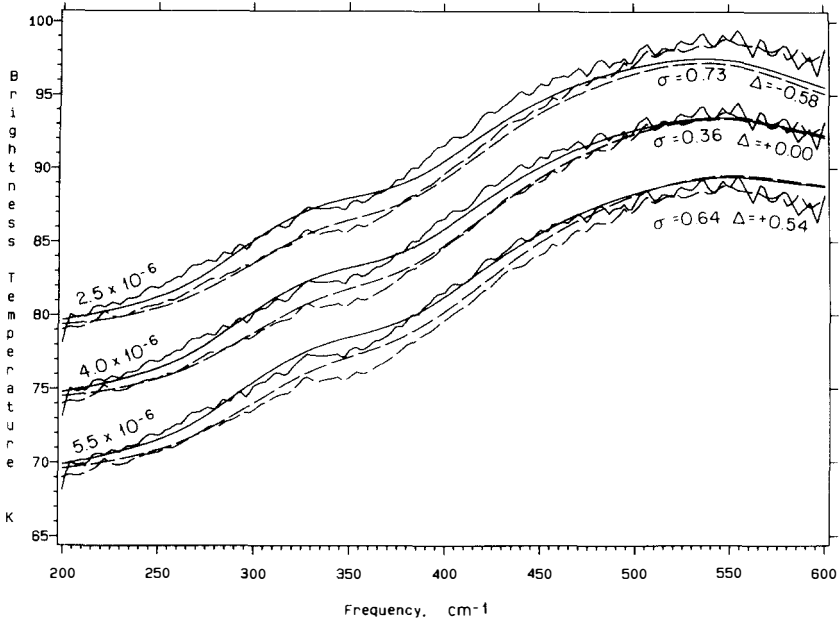


FIG. 9. Effect of varying haze quantity in Model A about the optimum value, holding CH_4 cloud abundance and H_2 mole fraction constant. The three sets of curves are labeled on the left by the haze column density in g cm^{-2} . (For explanation of lines and symbols see Fig. 8 caption.) Varying haze quantity by $\pm 40\%$ doubles the average RMS deviation. We determine a Titan tholin haze column density of $4 \pm 2 \times 10^{-6} \text{ g cm}^{-2}$ above the clouds.

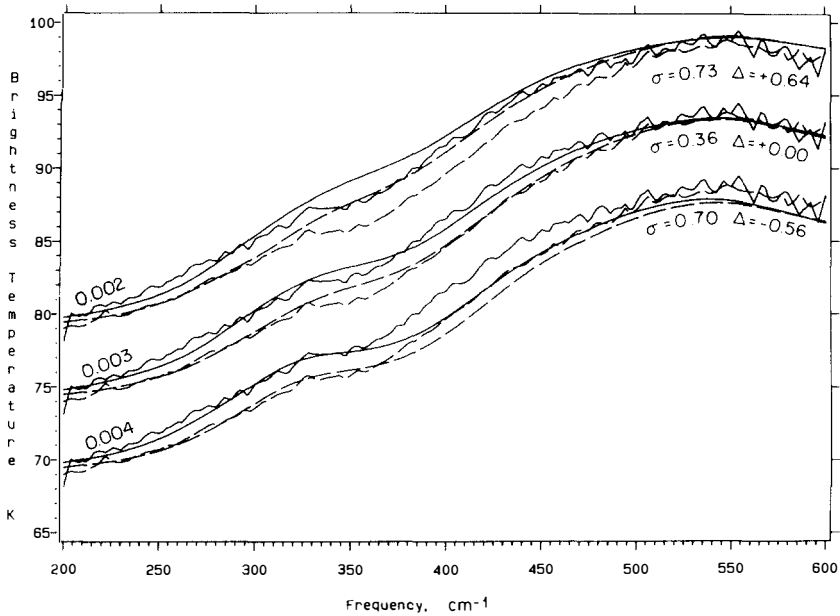


FIG. 10. Effect of varying H_2 mole fraction in Model A about the optimum value, holding haze column density and CH_4 cloud abundance constant. The three sets of curves are labeled on the left by the H_2 mole fraction. (For explanation of lines and symbols see Fig. 8 caption.) Varying H_2 mole fraction by ± 0.001 doubles the average RMS deviation, defining our range of 0.003 ± 0.001 .

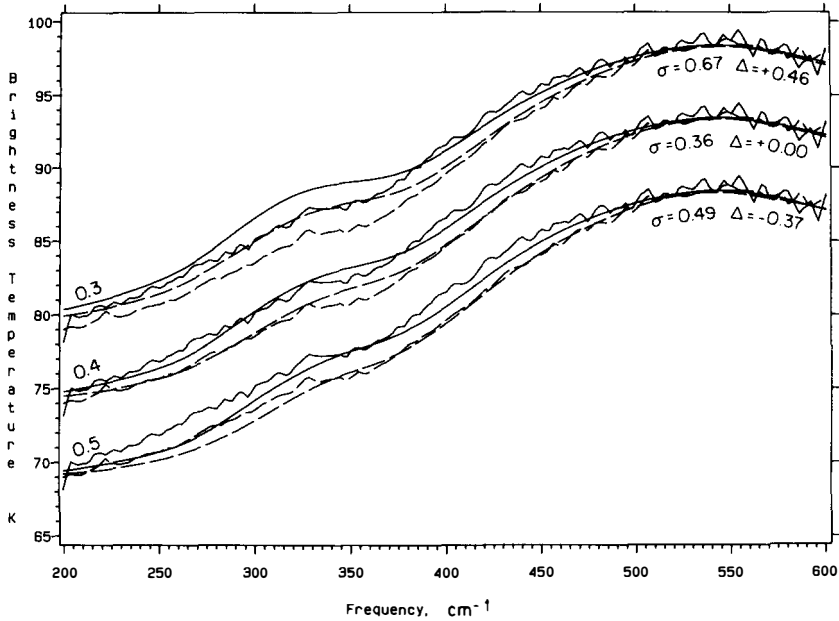


FIG. 11. Effect of varying CH₄ cloud mass density in Model A about the optimum value, holding haze column density and H₂ mole fraction constant. The three sets of curves are labeled on the left by the integrated CH₄ column density in g cm⁻². (For explanation of lines and symbols see Fig. 8 caption.) A decrease of the CH₄ cloud density by 25% doubles the average RMS deviation, while an increase by 25% increases the RMS deviation by a factor of 1.4. We determine a CH₄ column density of 0.4 ± 0.1 g cm⁻² since agreement below 300 cm⁻¹ is judged unacceptable for column densities above 0.5 g cm⁻².

uniform in altitude as in Fig. 8(B) or a multi-layer distribution as in Fig. 8(A), are both sufficient to match the observed Titan spectrum to a tolerance better than 0.5°K. We conclude that there *must* be about 0.1 g cm⁻² of cloud material near T_{\min} (between 2610 and 2625 km), and that there must be at lower altitudes a quantity of cloud which, when added to that in the layer above, produces a total column density of about 0.4 g cm⁻². We prefer to locate the lower layer(s) above 2590 km, since investigation has shown that, in a two-layer or uniform model, the fit with observations degrades when a substantial portion of the cloud lies below 2590 km. Within the above constraints, the cloud material may be distributed in various ways as long as the column density in lower-lying slabs is greater than, or equal to, that in the layer(s) near T_{\min} .

In the models with a uniform cloud distribution extending below 2590 km toward the

surface (e.g., Fig. 8(C), the shielding of the lower atmosphere by overlying cloud opacity allows the possibility of additional CH₄ condensate near the surface. Our calculations show, for example, that there is only a small difference in quality of fit to the observations between a condensed CH₄ mass fraction of 1×10^{-4} from 2620 to 2590 km, and one of 1×10^{-4} from 2620 km to the surface at 2575 km. Thus, one cannot exclude on the basis of thermal emission *alone* the presence of substantial CH₄ cloud below 2590 km.

3. Atmospheric CH₄ and Ar

Since the spectrum is not very sensitive to the CH₄ gas component, little can be said about its abundance except in an indirect way. The distribution of CH₄ cloud requires condensation by at most 2600 km, which in turn implies a methane gas mole fraction of at least 0.04, corresponding to a surface satu-

ration of about 35%. This lower limit is valid only for condensation of CH₄ to the pure state (see Discussion below).

The thermal emission properties of the atmosphere are rather insensitive to the argon content. Compared to a gas mixture with no Ar, the presence of ~15% Ar (estimated on the basis of bulk atmospheric molecular mass) will enhance the CH₄ gas phase absorption by ~20%, decrease the atmospheric N₂ absorption by ~2%, and leave the H₂ absorption unaffected (cf. Urbaniak *et al.*, 1976; Dagg *et al.*, 1974; Kiss and Welsh, 1959). Since condensed CH₄ dominates the gas phase CH₄ contribution, and the variation of N₂ absorption with Ar content is so small, the atmospheric Ar content is both undetermined and has insignificant impact on derived quantities and locations of other atmospheric constituents.

4. Surface Visibility

Surface visibility is investigated in more detail in Fig. 12. In Figs. 12a, b, and c are shown, for Models A, B, and C, the variation with frequency of the altitude of unit optical depth, or, alternatively, the surface optical depth τ_s , if $\tau_s < 1.0$. Results are shown for $\theta = 0^\circ$ (solid curves) and 60° (dashed curves), corresponding approximately to the Voyager average emission angles of 7.3 and 52.7°. As one would expect, altitudes of unit optical depth delineate, in a staircase fashion, the altitudes of methane cloud concentration, clearly reflecting in (a) the two layers of CH₄ cloud at 2620 to 2615 km and 2600 to 2595 km, and in (b) the single layer from 2615 to 2600 km. In (c) the cloud distribution is uniform in mass fraction from 2620 km downward, and the altitude of unit optical depth drops gradually with frequency due to decreasing CH₄ opacity. In all cases the influence of the H₂ absorption maxima at 366 and 610 cm⁻¹ can be seen. H₂ absorption is the dominant opacity source at $\bar{\nu} \geq 400$ cm⁻¹.

The minimum vertical ($\theta = 0^\circ$) optical depth is reached near 520 cm⁻¹. Here $\tau \approx 0.6$, so about 50% of the surface radiation

escapes through the overlying atmosphere. The observation that the brightness temperature is about equal to the surface temperature from 500 to 600 cm⁻¹ then implies that roughly equal amounts of radiance are contributed by the surface and the overlying atmosphere. At $\theta = 60^\circ$, the surface visibility is lower, with the unit optical depth altitude about 2 to 4 km above the surface. Thus, as noted earlier by Flasar *et al.* (1981), IRIS measurements near 530 cm⁻¹ yield information on the near-surface temperature. In addition, atmospheric transmission near this frequency is sufficiently high that variations in surface emissivity could be detected by measuring the longitudinal variation of T_B at near-normal emission.⁵ The only apparent obstacle to this atmospheric window near 19 μm is scattering by the CH₄ cloud. Since Mie scattering calculations show that the single scattering albedo $\bar{\omega}_0 = 0.25$ for 1- μm radius CH₄ cloud particles near $\lambda = 19 \mu\text{m}$, scattering is minor compared to CH₄ absorption and should not greatly degrade surface visibility except near the limb. This region of the infrared thus provides some opportunity for remote sensing of Titan's surface, otherwise possible only at $\lambda > 1 \text{ cm}$.

The results and limits determined above are summarized in Table I and Fig. 1.

DISCUSSION

In summary, we have found that the averaged Voyager IRIS Titan spectra from

⁵ The first such study has in fact been made (Flasar *et al.*, 1981). At a resolution of 30° in longitude, <1°K variation in T_B was found, with coverage most complete near the equator. Since the emissivities of Titan tholin [0.92 (Khare *et al.*, 1984)] and CH₄-rich mixtures [~ 0.98 (Pinkley *et al.*, 1978; Singh and Miller, 1978)] at 0° emission angle differ by 6%, a continental boundary would produce a 3% (about 3°K) jump in T_B near 530 cm⁻¹, where $\tau \approx 0.6$. Transitions between tholin and either H₂O ice, NH₃ ice, mixed ices, or CH₄ solutions should be detectable, and apparently are not found by Flasar *et al.* near Titan's equator at spatial scales ≈ 1400 km. (With T_B discrimination $\leq 0.5^\circ\text{K}$, H₂O ice/CH₄ solution boundaries should also be detectable.)

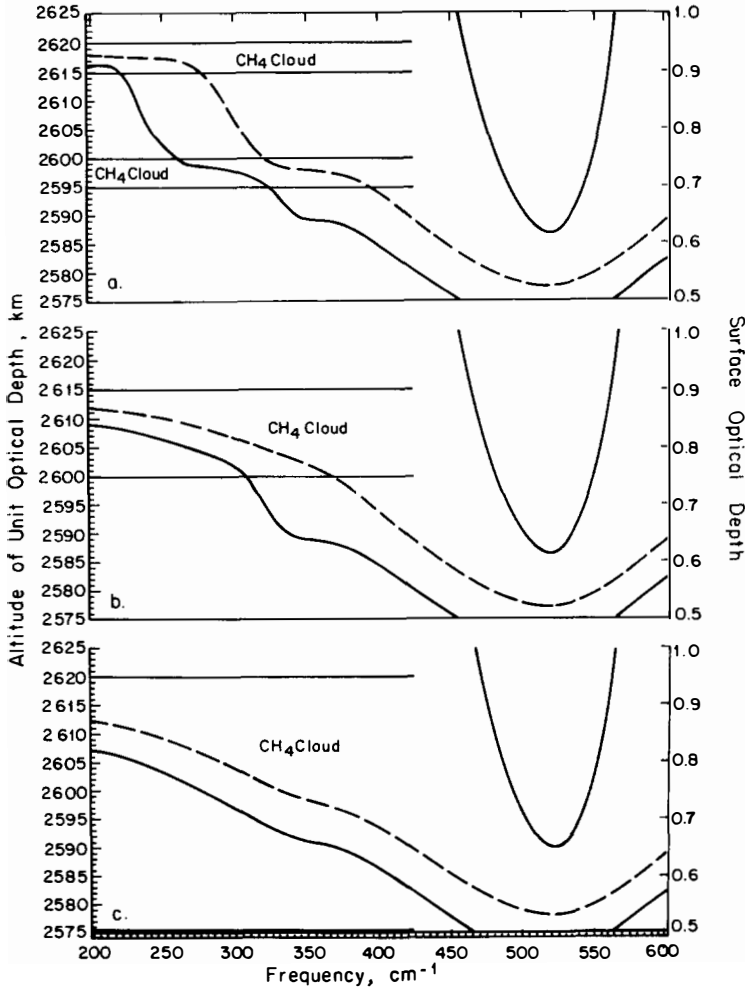


FIG. 12. Computed altitude of unit optical depth (solid and dashed lower curves: left legend) or optical depth at the surface (solid upper curve: right legend) as a function of frequency for Models A, B, and C (see text or Fig. 8 caption). The location of the CH₄ cloud in each model is delimited by the horizontal lines at left. Solid and dashed curves correspond respectively to emission angles of 0 and 60°. (These approximate the 7.3 and 52.7° emission angles for which observations and results have been compared.) Curves of unit optical depth tend to parallel the CH₄ cloud altitudes to varying degrees, depending on emission angle and cloud location. The minimum vertical optical depth is about 0.6 at 520 cm⁻¹.

200 to 600 cm⁻¹ at emission angles of 7.3 and 52.7° provide a rich source of information on Titan's tropospheric and mesospheric composition. We have determined the H₂ mole fraction in the troposphere to be 0.003 ± 0.001 , the condensed CH₄ column density above 2590 km to be 0.4 ± 0.1 g cm⁻², and the haze column density in the mesosphere to be $4 \pm 2 \times 10^{-6}$ g cm⁻².

About 0.1 g cm⁻² of the CH₄ condensate must be located near the atmospheric T_{\min} at $R \approx 2615$ km. CH₄ gas mole fraction in equilibrium with the highest allowable location of the lowermost cloud is ~ 0.04 . We now discuss the implications of, and some uncertainties in, these quantitative determinations, and compare our results with those of previous studies.

TABLE I
GAS, CLOUD AND HAZE IN TITAN'S ATMOSPHERE

Component	Phase	Location	Quantity	Notes
N ₂	Gas	Throughout	~81%	Major atmospheric constituent (Broadfoot <i>et al.</i> , 1981); N ₂ /Ar ratio adjusted to maintain average molecular weight of 28.6 (Samuelson <i>et al.</i> , 1981).
³⁶ Ar	Gas	Throughout	~15%	Inferred by atmospheric molecular weight and nebular condensation models (see Owen, 1982).
CH ₄	Gas	Troposphere below 2600 km	≥4%	Lower limit set by requirement of CH ₄ condensation at 2600 km or lower (see text).
		Mesosphere above 2625 km	~2%	Limited by vapor pressure at T_{\min} .
		Mesosphere above 3700 km	8%	EUV observations (Smith <i>et al.</i> , 1982).
H ₂	Gas	Troposphere	0.3 ± 0.1%	From IRIS spectral analysis [this work; Samuelson <i>et al.</i> (1981) give 0.2 ± 0.1%].
Organic haze	Solid	Mesosphere	4 ± 2 × 10 ⁻⁶ g cm ⁻²	This work. Must be in near-isothermal region above about 2750 km to provide brightness at $\bar{\nu} > 450$ cm ⁻¹ and preserve limb darkening.
		Troposphere	<5 × 10 ⁻⁴ g cm ⁻²	Upper limit for organic haze which may be mixed with liquid CH ₄ (not required).
Methane cloud	Liquid, solid?	Troposphere: 2610–2625 km	≈0.1 g cm ⁻²	This work. Upper cloud needed to produce sufficiently low T_B near 200 cm ⁻¹ .
		2590–2610 km	≈0.3 g cm ⁻²	Lower cloud provides proper spectral shape and maintains limb darkening.
		Below 2590 km	≤0.4 g cm ⁻²	Additional near-surface cloud is allowed but not required.

TROPOSPHERIC GAS PHASE CH₄ AND H₂

In obtaining the CH₄ gas abundance lower limit of 0.04, condensation of CH₄ to the pure state is assumed. Since the condensate is more likely a solution containing CH₄, C₂H₆, and N₂ (Lunine *et al.*, 1983), the equilibrium partial pressure of CH₄ will be lower, and the necessary mole fraction for condensation will be correspondingly reduced. Solution effects may reduce the lower limit on tropospheric CH₄ mole fraction to as little as ~0.02.

The H₂ mole fraction we derive, 0.003 ± 0.001, agrees within error with the value 0.002 ± 0.001 found by Samuelson *et al.*

(1981). Our preferred value 0.003 results from the use of temperature-dependent collision-induced absorption spectra based on experimental data at 77.4°K, much closer to relevant Titan temperatures than the 195°K laboratory spectrum used as the basis of the calculation of N₂-induced H₂ opacity by Samuelson *et al.* (1981). The accuracy of our spectra is limited only by that of the scaling relation (Ozier and Fox, 1970; Courtin, 1982) used to estimate H₂-N₂ opacity from the accurate computed H₂-H₂ spectra. Also, the explicit use of the CH₄ liquid spectrum, adjusted for temperature by the Birnbaum and Cohen theory, and the necessity of high altitude haze opacity, to-

gether force a tight constraint on the H₂ spectral contribution.

CH₄ CLOUD

1. Optical Depths

The vertical optical depth (τ_v) of CH₄ condensate ≈ 2 at 200 cm⁻¹, and that of organic haze ≈ 0.006 at 600 cm⁻¹, with a minimum total tropospheric optical depth ≈ 0.6 at 520 cm⁻¹. These values agree well with opacities derived by Samuelson *et al.* (1981): $\tau_{\text{tropopause}} \approx 3$ at 200 cm⁻¹ (including opacity from gaseous N₂ and CH₄; cf. Fig. 4), $\tau_v \approx 0.6$ at 530 cm⁻¹, and $\tau_{\text{mesosphere}} = 0.006$ at 600 cm⁻¹. (These values are for their 96°K surface temperature, high altitude haze model.) The cloud opacity we require is less than the residual opacity of $8 > \tau_{\text{cloud}} > 4$ found by Courtin (1982). Our requirement of the location of roughly 75% of the cloud mass between 2590 and 2610 km agrees well with the opacity peak between 2585 and 2610 km in the radiative equilibrium model of Samuelson (1983). His model requires a mean thermal-infrared optical depth of $3 < \tau_{\text{thermal}} < 9$. The maximum blackbody flux from a surface at 94°K occurs at 324 cm⁻¹, where $\tau_v \approx 2$ in our models. Our results are then more consistent with the lower limit of τ_{thermal} in Samuelson's model. Samuelson derives a fraction of solar energy reaching Titan's surface of 13 to 33% (corresponding respectively to a uniform mass fraction of cloud in the troposphere, or concentration of cloud at the tropopause). Since our models require that cloud opacity is distributed near and below T_{min} (not concentrated at the tropopause), solar input to Titan's surface is expected to be near the low end of the above range.

2. Cloud Distribution

Since a cloud distribution limited to altitudes above 2590 km is slightly favored, mild preference is given to the idea that a zone free of CH₄ cloud exists near Titan's surface. Subsaturation of CH₄ (with respect

to the pure liquid) near the surface is strongly indicated by detailed studies of the Voyager radio occultation temperature profile of the lower atmosphere (Eshleman *et al.*, 1983). While CH₄ subsaturation excludes the presence of large exposed surface areas of nearly pure liquid methane (Flasar, 1983), it is consistent with the multicomponent surface solution composed primarily of C₂H₆, CH₄, and N₂ proposed by Lunine *et al.* (1983). They predict an ethane-rich fog near the surface, with the condensation of a methane-rich liquid phase beginning at the 84°K level, which is coincident with the 2590-km level above which we prefer the cloud to be located. While Lunine *et al.* (1983) point out that the CH₄-C₂H₆ system forms a solid phase below 77°K, the presence of N₂ may maintain liquid hydrocarbon phases everywhere in Titan's atmosphere.

3. Condensate Phase and Composition

The condensation of a CH₄-N₂ gas mixture at $T > 63^\circ\text{K}$ often results in one or two *liquid* phases, depending on temperature, pressure, and the presence of other hydrocarbons such as C₂H₆ and C₃H₈ (Tsaturyants *et al.*, 1979). At 77.0°K and a total pressure of 0.814 bar, the condensation of N₂ with CH₄, C₂H₆, and C₃H₈ produces an N₂-rich lower liquid phase with about 2:1 N₂:CH₄ and a hydrocarbon-rich upper liquid phase with 10 mol % N₂ and roughly equal amounts of methane, ethane, and propane (Tsaturyants *et al.*, 1979). The N₂-rich phase retains a 2:1 molar ratio and remains liquid down to the N₂ freezing point of 63°K (Falk and Stoner, 1981). The 10 mol % N₂ found in the hydrocarbon-rich upper liquid phase will likely depress the binary CH₄-C₂H₆ solidification temperature of 77°K by several degrees. While the N₂ content will vary, and may be somewhat less in the Titanian cloud because of lower N₂ pressure ($p = 0.4$ bar at the 77°K level), any extension of the stability field of the liquid below 77°K makes a significant difference in the overall distribution of cloud material

between the liquid and solid states. This interesting problem should be addressed directly by laboratory experiments investigating the phase behavior of N_2 -hydrocarbon condensates through the temperature range 70–100°K and pressure range 0.1–1.6 bar.

While the condensation of some N_2 with CH_4 and C_2H_6 to form the cloud droplets makes it more likely that the cloud condensate is in the liquid state, it also produces an uncertainty in the deduced cloud mass through the introduction of additional N_2 opacity and modification of the CH_4 absorption strength because of liquid CH_4 - N_2 collisions. Computed spectra show that the absorption strength for CH_4 - N_2 collisions is roughly $\frac{1}{3}$ that of CH_4 - CH_4 collisions at these temperatures. Taking 0.40 g cm^{-2} as the nominal CH_4 cloud column density, an N_2 mole fraction of 0.2, for example, would reduce the CH_4 bulk absorption coefficient to 0.87 of that in pure CH_4 , and thus require 1.15 times the CH_4 column density (0.46 g cm^{-2}) and 1.35 times the total cloud column density (0.62 g cm^{-2}). The column density of liquid-state N_2 is at most about 10^{-3} of that of gaseous N_2 above 2590 km, so the N_2 opacity of the condensate should not significantly affect the computed spectrum at these frequencies.

The strength and band shape of C_2H_6 collision-induced absorption (Arning *et al.*, 1981) is sufficiently similar to that of CH_4 that part of the detected cloud mass could be C_2H_6 . Since the vapor pressure of ethane in the proposed surface ocean is very low compared to that of methane (Lunine *et al.*, 1983), we expect the contribution of C_2H_6 to the total opacity to be small.

4. Scattering and Cloud Particle Size

As mentioned above, our study excludes scattering. Mie scattering calculations using the optical constants of liquid CH_4 and Titan tholin show that the nonscattering approach employed is quantitatively valid for $\lambda \geq 17 \mu\text{m}$, for tholin particles up to radius $r \approx 5 \mu\text{m}$, and for CH_4 cloud droplets up to $r \approx 1.5 \mu\text{m}$. The particle growth and sedi-

mentation model of Toon *et al.* (1980) indicates that organic haze particles are probably always smaller than the $5\text{-}\mu\text{m}$ limit. The main concern is then the size of the cloud condensate particles. Since Titan's atmosphere appears to be in radiative equilibrium except for the lowest 4 km (Eshleman *et al.*, 1983), strong vertical transport is unlikely, and CH_4 condensate particles at the indicated altitudes may be small.

The observations in fact indicate that scattering is not a dominant process in Titan's atmosphere at thermal wavelengths. As cloud particles become scattering, the emissivity of the cloud decreases, the T_B falls below the true physical temperature, and substantial limb darkening results (van de Hulst, 1980, Sect. 18.6). Let us take as an example CH_4 droplets of $r = 5 \mu\text{m}$ at $\bar{\nu} = 200 \text{ cm}^{-1}$. The deflection angle of a single scattering event is Φ and the angle of emission with respect to the local normal is $\theta \equiv \cos^{-1}\mu$. Mie scattering calculations (which we have performed for CH_4 particles of $0.1 \mu\text{m} \leq r \leq 5.0 \mu\text{m}$, at $100 \text{ nm} \leq \lambda \leq 1 \text{ mm}$) show that the asymmetry parameter $g = \langle \cos \Phi \rangle \approx 0.1$, and the single scattering albedo $\bar{\omega}_0 \approx 0.97$ in this case. The emissivity $E(\theta)$ of a slab of these particles of substantial optical depth (using the approximation of a Henyey-Greenstein phase function) varies substantially with emission angle: $E(0^\circ) \approx 0.50$ while $E(60^\circ) \approx 0.35$ (cf. van de Hulst, 1980, Sects. 18.6, 11.1–2). As a result, if scattering were important one should see a limb darkening of as much as 9°K at 200 cm^{-1} , while only $\sim 1^\circ\text{K}$ is observed.

The combination of minimal limb darkening and low T_B near 200 cm^{-1} implies that the observed radiance is from a slab of particles of high emissivity—or equivalently low $\bar{\omega}_0$ —at physical temperature $T = T_B$. The observed magnitude of the limb darkening, through analysis of the kind outlined above, allows us to set a tentative upper bound on cloud particle radius: $r_{CH_4} \leq 2 \mu\text{m}$.

The only placement of particles larger

than this consistent with the observations would be *above* the temperature minimum, such that scattering, which produces limb darkening even in an isothermal atmosphere, is offset by an increase of temperature with depth, which in the absence of scattering would produce limb brightening. Rather large particles of C₂H₆, C₃H₈, and other abundant products of atmospheric organic synthesis condensing above T_{\min} (Sagan and Thompson, 1984) may therefore contribute some of the thermal opacity without *necessarily* producing disagreement with the observations.

The fact that the high frequency portion of the spectrum shows a relatively high T_B is further evidence for the absence of larger CH₄ cloud particles. For physically plausible particle sizes the scattering efficiency Q_s increases with frequency. (This is because of the trend characteristic of passage from the Rayleigh domain where $r/\lambda \ll 1$ to the geometric domain where $r/\lambda \gg 1$.) If the surface were surmounted by a near conservatively scattering cloud of substantial optical depth, the T_B of the surface (at $T_{\text{physical}} = 93^\circ\text{K}$) would be at most 74°K , much lower than observed. In addition, the amount of limb darkening near 530 cm^{-1} would be much greater than observed.

If *some* particles with radii near the $2\text{-}\mu\text{m}$ limit are present, their main effect will be a bias of detected thermal radiation toward the upper regions of the cloud. This would reduce the quantity of condensate required at higher altitudes, and allow an increase of

the quantity of cloud material at lower altitudes (below 2610 km).

At visual frequencies the CH₄ absorption is low and r/λ is much greater. The scattering optical depth is then very large: $\sim 10^4$ for particles of $r = 1\ \mu\text{m}$ in the geometric limit. The implications of the presence of this optically thick, but inherently conservative cloud ($\bar{\omega}_0 > 0.9999999$ for $220\text{ nm} < \lambda < 2\ \mu\text{m}$, and $r = 1\ \mu\text{m}$) are further discussed in Sagan and Thompson (1984).

5. CH₄ Content: Gas, Cloud, and Surface

It is interesting to compare the amount of cloud in Titan's atmosphere with that in Earth's. The column density of a gaseous component is $L = (\mu_i X_i / \mu) L_{\text{total}} = (\mu_i X_i / \mu) p / g$, where μ_i is the molecular mass of a component present at mole fraction X_i , μ is the atmospheric molecular mass, L_{total} is the total atmospheric column density, p the total pressure and g the local gravitational acceleration. We take for Titan $X_{\text{CH}_4} = 0.03$, $p = 1.6 \times 10^6\text{ dyn cm}^{-2}$, and $g = 135\text{ cm sec}^{-2}$. The average tropospheric water content on Earth is about 2 g m^{-3} , equally divided between cloud particles of $r_{\text{avg}} \approx 10\ \mu\text{m}$ and raindrops of $r_{\text{avg}} \approx 1\text{ mm}$ (Ludlam, 1980), while the total mass of atmospheric water vapor is $1.7 \pm 0.1 \times 10^{19}\text{ g}$ (Walker, 1977). The quantities of vapor and cloud on Earth and Titan computed from these values are compared in Table II. The Titan: Earth ratios show that while Titan has about one-fourth the average cloud column density, it has about 60 times more vapor (for the adopted CH₄ mole fraction of 0.03), and therefore has a cloud:gas ratio only 0.004 of Earth's. Since Titan's troposphere seems much more stable against convection than Earth's (Eshleman *et al.*, 1983) this result is probably not surprising.

The eccentricity of Titan's orbit indicates that there must either be no substantial ocean, or a deep global ocean free of substantial land masses (Sagan and Dermott, 1982). Accordingly, we point out that current data strongly suggest either a deep global C₂H₆-CH₄-N₂ ocean (Lunine *et al.*,

TABLE II

VAPOR AND CLOUD CONDENSATES ON TITAN AND EARTH, MEAN VALUES

Planet	Condensate	Column density (g cm ⁻²)		Ratio cloud/gas
		Cloud	Gas	
Earth	H ₂ O	1.7	3.3	0.5
Titan	CH ₄	0.4	200	0.002
Titan/Earth		0.25	60	0.004

1983; Dermott *et al.*, 1984) with no substantial land masses, or, if C_2H_6 is destroyed over geologic time by near-surface processes [for example, cosmic ray processing; see Capone *et al.* (1983) and Sagan and Thompson (1984)], a solid surface with at most lakes of liquid solution. In the latter case, CH_4 -rich organic rainfall on Titan may participate in erosional and transport processes of accumulated surface organics, and the solution and dissolution of sparingly soluble organic compounds will produce crystalline and sedimentary deposits in subsurface and perhaps lakeshore locations.

REMAINING DIFFERENCES

Notable residual differences exist between the Voyager average spectra and those computed. Much of the small-scale structure in the region $200\text{--}600\text{ cm}^{-1}$ is due to vibrational-rotational transitions of molecular sources in the mesosphere. Several such features, which are noticeable but relatively weak at lower latitudes, are sufficiently strong at high latitudes to allow unique identification (Maguire *et al.*, 1981; Kunde *et al.*, 1981). Since our thermal emission model includes only rotational transitions of N_2 , CH_4 , and H_2 (plus haze opacity), it will reproduce (at best) the "continuum" on which these sharper molecular emission features are superposed. Mesospheric emission by C_3H_4 (propyne) in particular accounts for at least part of the discrepancy near 350 cm^{-1} (see Maguire *et al.*, 1981, Fig. 1), where the inflection seems stronger in the observed than in the computed spectra. An attempt to better reproduce the observed inflection by simply increasing the H_2 abundance (Fig. 10) fails: This adds too much opacity in the lower atmosphere and results in a poor fit above 350 cm^{-1} .

Even if the fine structure is ignored, one can note ways in which the spectra could be better matched. At $230\text{--}280$ and $370\text{--}470\text{ cm}^{-1}$, the computed line for $\theta = 7.3^\circ$ seems systematically too low: the real atmosphere

is more limb darkened than computations would indicate. After our model computations and most analysis were completed, a revised atmospheric structure, obtained through detailed analysis of the Voyager radio occultation data, became available (Lindal *et al.*, 1983). The most relevant differences between the Lindal *et al.* structure and that used here seem to be (1) the temperature profile is 1 to 2°K cooler from the temperature minimum down to a few km above the surface; (2) the temperature gradient $|dT/dz|$ is slightly lower in this region; and (3) $|dT/dz|$ is greater in the lowermost few km of atmosphere. A higher temperature gradient near the surface would enhance limb darkening from atmospheric sources (mostly CH_4 and H_2), and thus result in greater limb darkening in the computed spectra. Observations would then be better matched, especially at $370\text{--}470\text{ cm}^{-1}$, where cloud and haze opacity are low and the conditions of the lower atmosphere significantly influence the spectra.

Additionally, the generally lower temperatures at cloud altitudes would result in a small reduction of the required column density of condensed CH_4 , since this opacity is required primarily to match the marked decrease of T_B toward 200 cm^{-1} . In order to maintain limb darkening at the lower frequencies, a similar distribution of cloud over altitude would still be required.

OBSERVATIONAL SUGGESTIONS

1. *In Situ Studies*

Whatever the fate of cloud precipitates, Titan may be the first body beyond the Earth to display global atmospheric transport of a volatile liquid. It is a world of particular interest for further study. Direct measurement of cloud particle sizes, number density, and composition should be a primary objective of a Titan atmospheric entry probe. A substantial flexibility and sophistication of analytical techniques is warranted, given the evidence for a great variety and chemical complexity of hazes and

clouds at various altitudes in Titan's atmosphere (see Sagan and Thompson, 1984).

2. Remote Sensing of the Troposphere and Surface

Remote radio observations currently lack the precision and disk resolution needed to provide the kind of accurate brightness measurements which would be most useful in a further study of surface/atmosphere/cloud/haze emission properties. However, disk-integrated measurements at shorter wavelengths could be valuable, and several opportunities exist for further studies of the Titanian thermal spectrum using Earth-based or Earth-orbiting facilities.

As noted in the previous discussion of surface visibility, infrared coverage or imaging at spatial resolution finer than the ~1400 km achieved to date could reveal boundaries between any one of H₂O ice, NH₃ ice, or CH₄ solution, and tholin. The temperature jump expected at such boundaries is 2–3°K for 50% atmospheric transmission. The detection of transitions between H₂O ice and either CH₄ solutions or NH₃-rich ice can be achieved with slightly better T_B discrimination. We are currently investigating in greater detail the thermal emission and radar reflection properties of plausible Titanian surfaces.

Of particular interest would be precise far-infrared observations extending from the Voyager low-frequency cutoff of about 200 cm⁻¹ (50 μm) through submillimeter to millimeter wavelengths. Cloud opacity should continue to predominate through 100 cm⁻¹ (100 μm), while atmospheric opacity dominates from ~70 cm⁻¹ (150 μm) through millimeter wavelengths (Fig. 3). N₂ opacity raises the $\tau = 1$ level to highest altitudes in the upper troposphere at $\bar{\nu} \approx 16$ cm⁻¹ ($\lambda \approx 0.6$ mm), beyond which the effective emission altitude is expected to return slowly toward the surface with increasing wavelength.

Atmospheric opacity gradually becomes negligible beyond cm wavelengths: this is the only spectral region where Titan's sur-

face is fully visible to external observation. Accurate radio interferometry could yield the limb darkening behavior of the surface, which is determined by its composition (dielectric constant) and surface texture (roughness and slope).

ACKNOWLEDGMENTS

We thank Frank Drake for his stimulus at a very early stage of this study and his continuing interest. B. N. Khare and co-workers for the use of Titan tholin optical constants prior to publication, and S. W. Squyres, G. Birnbaum, R. E. Samuelson, V. Eshleman, G. L. Tyler, P. Gierasch, R. Courtin, J. Pearl, J. I. Lunine, D. J. Stevenson, and K. Rages for valuable discussions. We are also grateful to Cornell Computer Services for support of scientific computing through special rates and grants, and acknowledge with thanks use of the Cornell/NASA Spacecraft Planetary Imaging Facility. The work was supported by NASA Grants NGL 33-010-082 and NGR 33-010-220.

REFERENCES

- ALLEN, D. A., AND T. L. MURDOCK (1971). Infrared photometry of Saturn, Titan, and the rings. *Icarus* **14**, 1–2.
- ALLEN, M., J. P. PINTO, AND Y. L. YUNG (1980). Titan: Aerosol photochemistry and variations related to the sunspot cycle. *Astrophys. J.* **242**, L125–L128.
- ARNING, H.-J., K. TIBULSKI, AND T. DORFMULLER (1981). Collision-induced spectra of simple liquids. *Ber. Bunsenges. Phys. Chem.* **85**, 1068–1071.
- BIRNBAUM, G. (1975). Far infrared collision-induced spectrum in gaseous methane. I. Band shape and temperature dependence. *J. Chem. Phys.* **62**, 59–62.
- BIRNBAUM, G. (1978). Far-infrared absorption in H₂ and H₂-He mixtures. *J. Quant. Spectrosc. Radiat. Transfer* **19**, 51–62.
- BIRNBAUM, G., AND E. R. COHEN (1976). Theory of line shape in pressure-induced absorption. *Can. J. Phys.* **54**, 593–602.
- BRIGGS, F. H. (1974). The radio brightness of Titan. *Icarus* **22**, 48–50.
- BROADFOOT, A. L., B. R. SANDEL, D. E. SHEMANSKY, J. B. HOLBERG, G. R. SMITH, D. F. STROBEL, J. C. MCCONNELL, S. KUMAR, D. M. HUNTEN, S. K. ATREYA, T. M. DONAHUE, H. W. MOOS, J. L. BERTAUX, J. E. BLAMONT, R. B. POMPHREY, AND S. LINICK (1981). Extreme ultraviolet observations from Voyager 1 encounter with Saturn. *Science (Washington, D.C.)* **212**, 206–211.
- BUONTEMPO, U., S. CUNSOLO, AND G. JACUCCI (1975). The far infrared absorption spectrum of N₂ in the gas and liquid phases. *J. Chem. Phys.* **63**, 2570–2576.
- CALDWELL, J. (1977). Thermal radiation from Titan's

- atmosphere. In *Planetary Satellites* (J. A. Burns, Ed.). Univ. of Arizona Press, Tucson.
- CAPONE, L. A., J. DUBACH, S. S. PRASAD, AND R. C. WHITTEN (1983). Galactic cosmic rays and N_2 dissociation on Titan. *Icarus* **55**, 73–82.
- COURTIN, R. (1982). The spectrum of Titan in the far-infrared and microwave regions. *Icarus* **51**, 466–475.
- DAGG, I. R., G. E. REESOR, AND J. L. URBANIAK (1974). Collision induced microwave absorption in N_2 , CH_4 , and N_2 -Ar, N_2 - CH_4 mixtures at 1.1 and 2.3 cm^{-1} . *Can. J. Phys.* **52**, 821–829.
- DANIELSON, R. E., J. J. CALDWELL, AND D. R. LARACH (1973). An inversion in the atmosphere of Titan. *Icarus* **20**, 437–443.
- DERMOTT, S. F., P. GIERASCH, J. GRADIE, C. SAGAN, AND W. R. THOMPSON (1984). Origin and depth of Titan's hydrocarbon ocean. In *Lunar and Planetary Science XV*, Part 1, pp. 222–223. Lunar and Planetary Institute, Houston.
- ESHLEMAN, V. R., G. F. LINDAL, AND G. L. TYLER (1983). Is Titan wet or dry? *Science (Washington, D.C.)* **221**, 53–55.
- FALK, M., AND R. STONER (1981). Possible layered structure in liquid CH_4 - N_2 mixtures. *J. Phys. C* **14**, L65–L67.
- FLASAR, F. M. (1983). Oceans on Titan? *Science (Washington, D.C.)* **221**, 55–57.
- FLASAR, F. M., R. E. SAMUELSON, AND B. J. CONRATH (1981). Titan's atmosphere: Temperature and dynamics. *Nature* **292**, 693–698.
- FROIDEVAUX, L., AND A. P. INGERSOLL (1980). Temperatures and optical depths of Saturn's rings and a brightness temperature for Titan. *J. Geophys. Res.* **85**, 5929–5936.
- GILLETT, F. C. (1975). Further observations of the 8–13 micron spectrum of Titan. *Astrophys. J.* **201**, L41–L43.
- GILLETT, F. C., W. J. FORREST, AND K. M. MERRILL (1973). 8–13 micron observations of Titan. *Astrophys. J.* **184**, L93–L95.
- HANEL, R., B. CONRATH, F. M. FLASAR, V. KUNDE, W. MAGUIRE, J. PEARL, J. PIRRAGLIA, R. SAMUELSON, D. CRUIKSHANK, D. GAUTIER, P. GIERASCH, L. HORN, AND C. PONNAMPERUMA (1982). Infrared observations of the Saturnian system from Voyager 2. *Science (Washington, D.C.)* **215**, 544–548.
- HANEL, R., B. CONRATH, F. M. FLASAR, V. KUNDE, W. MAGUIRE, J. PEARL, J. PIRRAGLIA, R. SAMUELSON, L. HERATH, M. ALLISON, D. CRUIKSHANK, D. GAUTIER, P. GIERASCH, L. HORN, R. KOPPANY, AND C. PONNAMPERUMA (1981). Infrared observations of the Saturnian system from Voyager 1. *Science (Washington, D.C.)* **212**, 192–200.
- HUNT, J. L., J. D. POLL, D. GOORVITCH, AND R. H. TIPPING (1983). Collision-induced absorption in the far infrared spectrum of Titan. *Icarus* **55**, 63–72.
- HUNTEN, D. M. (1978). A Titan atmosphere with a surface temperature of 200K. In *The Saturn System* (D. M. Hunten and D. Morrison, Eds.), NASA Conference Publ. CP-2068. NASA, Washington, D.C.
- JAFFE, W., J. CALDWELL, AND T. OWEN (1980). Radius and brightness temperature observations of Titan at centimeter wavelengths by the Very Large Array. *Astrophys. J.* **242**, 806–811.
- KHARE, B. N., C. SAGAN, E. T. ARAKAWA, F. SUITS, T. A. CALLCOTT, AND M. W. WILLIAMS (1984). Optical constants of organic tholins produced in simulated Titanian atmospheres: From soft X-ray to microwave frequencies. *Icarus* **60**, 127–137.
- KISS, Z. J., AND H. L. WELSH (1959). The pressure-induced rotational absorption spectrum of hydrogen. II. Analysis of the absorption profiles. *Can. J. Phys.* **37**, 1249–1259.
- KUNDE, V. G., A. C. AIKIN, R. A. HANEL, D. E. JENNINGS, W. C. MAGUIRE, AND R. E. SAMUELSON (1981). C_4H_2 , HC_3N and C_2N_2 in Titan's atmosphere. *Nature* **292**, 686–688.
- LINDAL, G. F., G. E. WOOD, H. B. HOTZ, D. N. SWEETNAM, V. R. ESHLEMAN, AND G. L. TYLER (1983). The atmosphere of Titan: An analysis of the Voyager 1 radio occultation measurements. *Icarus* **53**, 348–363.
- LOEWENSTEIN, R. F., D. A. HARPER, R. H. HILDEBRAND, H. MOSELEY, E. SHAYA, AND J. SMITH (1980). Far-infrared photometry of Titan and Iapetus. *Icarus* **43**, 283–287.
- LOW, F. J. (1965). Planetary radiation at infrared and millimeter wavelengths. *Lowell Obs. Bull.* **6**, 184–187.
- LOW, F. J., AND G. H. RIEKE (1974). Infrared photometry of Titan. *Astrophys. J.* **190**, L143–L145.
- LUDLAM, F. H. (1980). *Clouds and Storms. The Behavior and Effect of Water in the Atmosphere*, Appendix 1.1. Penn State Univ. Press, University Park.
- LUNINE, J. I., D. J. STEVENSON, AND Y. L. YUNG (1983). Ethane ocean on Titan. *Science (Washington, D.C.)* **222**, 1229–1230.
- MAGUIRE, W. C., R. A. HANEL, D. E. JENNINGS, V. G. KUNDE, AND R. E. SAMUELSON (1981). C_3H_8 and C_3H_4 in Titan's atmosphere. *Nature* **292**, 683–686.
- MCCARTHY, J. F., J. B. POLLACK, J. R. HOUCK, AND W. J. FORREST (1980). 16–30 micron spectroscopy of Titan. *Astrophys. J.* **236**, 701–705.
- MORRISON, D., D. P. CRUIKSHANK, AND R. E. MURPHY (1972). Temperatures of Titan and the Galilean satellites at 20 microns. *Astrophys. J.* **173**, L143–L146.
- OWEN, T. (1982). The composition and origin of Titan's atmosphere. *Planet. Space Sci.* **30**, 833–838.
- OZIER, I., AND K. FOX (1970). Theory of the collision-induced rotational spectrum of tetrahedral molecules. *J. Chem. Phys.* **52**, 1416–1430.
- PINKLEY, L. W., P. P. SETHNA, AND D. WILLIAMS

- (1978). Optical constants of liquid methane in the infrared. *J. Opt. Soc. Am.* **68**, 186–189.
- POLLACK, J. B. (1973). Greenhouse models of the atmosphere of Titan. *Icarus* **19**, 43–58.
- ROELIG, T. L., D. J. ENNIS, AND J. R. HOUCK (1981). The 1-mm brightness temperature of Titan. *Icarus* **45**, 618–623.
- SAGAN, C. (1973). The greenhouse of Titan. *Icarus* **18**, 649–656.
- SAGAN, C., AND S. F. DERMOTT (1982). The tide in the seas of Titan. *Nature* **300**, 731–733.
- SAGAN, C., AND B. N. KHARE (1979). Tholins: Organic chemistry of interstellar grains and gas. *Nature* **277**, 102–107.
- SAGAN, C., AND B. N. KHARE (1981). The organic clouds of Titan. *Bull. Amer. Astron. Soc.* **13**, 701.
- SAGAN, C., B. N. KHARE, AND J. LEWIS (1984). Organic matter in the Saturn system. In *Saturn* (T. Gehrels and M. S. Matthews, Eds.), University of Arizona Press, Tucson.
- SAGAN, C., AND W. R. THOMPSON (1984). Production and condensation of organic compounds in the atmosphere of Titan. *Icarus* **59**, 133–161.
- SAMUELSON, R. E. (1983). Radiative equilibrium model of Titan's atmosphere. *Icarus* **53**, 364–387.
- SAMUELSON, R. E., R. A. HANEL, V. G. KUNDE, AND W. C. MAGUIRE (1981). Mean molecular weight and hydrogen abundance of Titan's atmosphere. *Nature* **292**, 688–693.
- SAVOIE, R., AND R. P. FOURNIER (1970). Far-infrared spectra of condensed methane and methane-d₄. *Chem. Phys. Lett.* **7**, 1–3.
- SINGH, S. P., AND R. C. MILLER (1978). Compressed-liquid dielectric constants and derived excess volumes for simple liquid mixtures: N₂ + CH₄ and Ar + CH₄. *J. Chem. Thermodyn.* **10**, 747–763.
- SMITH, G. R., D. F. STROBEL, A. L. BROADFOOT, B. R. SANDEL, D. E. SHEMANSKY, AND J. B. HOLBERG (1982). Titan's upper atmosphere: Composition and temperature from the EUV solar occultation results. *J. Geophys. Res.* **87**, 1351–1360.
- STROBEL, D. F. (1982). Chemistry and evolution of Titan's atmosphere. *Planet. Space Sci.* **30**, 839–848.
- THOMPSON, W. R., AND C. SAGAN (1981). The microwave spectrum of Titan: Compatibility with post-Voyager atmospheric models. *Bull. Amer. Astron. Soc.* **13**, 703.
- TOON, O. B., R. P. TURCO, AND J. B. POLLACK (1980). A physical model of Titan's clouds. *Icarus* **43**, 260–282.
- TSATURYANTS, A. B., YU. I. KHMARA, V. M. YAGODIN, V. A. NIKOL'SKII, AND A. V. MOSTITSKII (1979). Use of Schroeder's equation for calculation of liquid-solid equilibria (of solutions of light paraffins and nitrogen). *Teplofiz. Teplotekh.* **37**, 63–65.
- TYLER, G. L., V. R. ESHLEMAN, J. D. ANDERSON, G. S. LEVY, G. F. LINDAL, G. E. WOOD, AND T. A. CROFT (1981). Radio science investigations of the Saturn system with Voyager 1: Preliminary results. *Science (Washington, D.C.)* **212**, 201–206.
- URBANIAK, J. L., G. E. REESOR, AND I. R. DAGG (1976). Microwave absorption in compressed CF₄, CH₄, and CF₄-Ar, CH₄-Ar mixtures in the 2.3 cm⁻¹ region. *Canad. J. Phys.* **54**, 1606–1612.
- VAN DE HULST, H. C. (1980). *Multiple Light Scattering: Tables, Formulas, and Applications*, Vol. 2. Academic Press, New York.
- WALKER, J. C. G. (1977). *Evolution of the Atmosphere*, Table 1.2. MacMillan Co., New York.
- YUNG, Y. L., M. ALLEN, AND J. P. PINTO (1984). Photochemistry of the atmosphere of Titan: Comparison between model and observations. *Astrophys. J. Suppl.* **55**, 465–506.